International Journal of Nanomedicine

Dovepress
open access to scientific and medical research

Open Access Full Text Article

ORIGINAL RESEARCH

# Pharmacokinetic parameters and tissue distribution of magnetic $Fe_3O_4$ nanoparticles in mice



This article was published in the following Dove Press journal:
International Journal of Nanomedicine
12 October 2010
Number of times this article has been viewed

Jun Wang[1]
Yue Chen[1]
Baoan Chen[1]
Jiahua Ding[1]
Guohua Xia[1]
Chong Gao[1]
Jian Cheng[1]
Nan Jin[1]
Ying Zhou[1]
Xiaomao Li[1]
Meng Tang[2]
Xue Mei Wang[2]

[1]Department of Hematology, Zhongda Hospital, Clinical Medical School, Southeast University, Nanjing, People's Republic of China; [1]Department of Physics, University of Saarland, D-266041 Saarbruechen, Germany; [2]National Key Laboratory of Bioelectronics (Chien-Shiung Wu Laboratory), Southeast University, Nanjing, People's Republic of China

Correspondence: Baoan Chen
Department of Hematology, The Affliated Zhongda Hospital, Southeast University, Nanjing 210009, People's Republic of China
Tel +86 25 8327 2006
Fax +86 25 8327 2011
Email cba8888@hotmail.com

**Background:** This study explored the pharmacokinetic parameters and tissue distribution of magnetic iron oxide nanoparticles ($Fe_3O_4$ MNPs) in imprinting control region (ICR) mice.

**Methods:** The $Fe_3O_4$ MNPs were synthesized by chemical coprecipitation, and their morphology and appearance were observed by transmission electron microscopy. ICR mice were divided into a control group and a $Fe_3O_4$ MNP-treated group. Probable target organs in ICR mice were observed, and the pharmacokinetic parameters and biodistribution of $Fe_3O_4$ MNPs in tissues were identified using atomic absorption spectrophotometry.

**Results:** $Fe_3O_4$ MNPs were spherical with a well distributed particle diameter, and were distributed widely in various target organs and tissues including the heart, liver, spleen, lungs, kidneys, brain, stomach, small intestine, and bone marrow. The majority of $Fe_3O_4$ MNPs were distributed to the liver and the spleen. $Fe_3O_4$ MNP levels in brain tissue were higher in the $Fe_3O_4$ MNP-treated group than in the control group, indicating that $Fe_3O_4$ MNPs can penetrate the blood–brain barrier.

**Conclusion:** These results suggest that the distribution of $Fe_3O_4$ MNPs was mostly in the liver and spleen, so the curative effect of these compounds could be more pronounced for liver tumors. Furthermore, $Fe_3O_4$ MNPs might be used as drug carriers to overcome physiologic barriers.

**Keywords:** magnetic nanoparticles, $Fe_3O_4$, tissue distribution, mice

## Introduction

With the development of nanotechnology, magnetic nanoparticles have shown application prospects since the 1970s.[1] Much attention has been paid over the past few years to the study of magnetic nanoparticles due to their particularly large surface-to-volume ratio, quantum size effect, and magnetic character, as well as their potential application in the areas of bioscience and medicine. Recently, magnetic nanoparticles have been used more and more frequently in biomedical and biotechnology studies, including targeted drug delivery, tumor magnetic hyperthermia therapy, contrast enhancement of magnetic resonance imaging, biosensors, rapid separation in environmental biology, and concentration tracing of specific targets, such as bacteria, leukocytes, and proteins.[2] So far, the magnetic nanoparticles with clinical applications are mainly composed of magnetic iron oxide, which has good chemical stability, magnetic responsiveness, and biocompatibility, in addition to possessing the general characteristics of nanoparticles. Moreover, iron oxide nanoparticles are the only magnetic nanomaterials approved for clinical use by the US Food and Drug Administration (FDA),[3,4] and the preparation method is relatively simple.

submit your manuscript | www.dovepress.com
Dovepress
DOI: 10.2147/IJN.S13662

In our previous studies,[5,6] we have demonstrated that $Fe_3O_4$ MNPs combined with chemotherapeutic drugs can inhibit tumor proliferation and induce apoptosis of tumor cells in a dose- and time-dependent manner, which may be related to changes in drug formulation caused by the magnetic nanomaterials. However, the in vivo metabolic processes of $Fe_3O_4$ MNPs within the organism, as well as their distribution in the important organ tissues, are as yet not completely understood.[7] Using chemical coprecipitation to synthesis $Fe_3O_4$ MNPs, we selected imprinting control region (ICR) mice as an investigative model. The mice were given the $Fe_3O_4$ NMPs by the intragastric route in view of the application perspective of $Fe_3O_4$ NMPs, and the concentrations of $Fe_3O_4$ MNPs in different organs and tissues were measured at particular time points using atomic absorption spectrophotometry. The pharmacokinetic parameters and biodistribution of $Fe_3O_4$ MNPs in tissues and the probable target organs in mice were determined to provide theoretic evidence for follow-up research and clinical application.

# Materials and methods

## Animals

ICR mice (6–8 weeks of age) weighing 18–22 g were used for the pharmacokinetic and tissue distribution studies, and were purchased from the Experimental Animal Center at Nantong University (Animal Certificate of Conformity SCXK 2008-0010). All animal experiments were evaluated and approved by the Animal and Ethics Review Committee of the Southeast University. The mice were kept at a room temperature controlled at 22° with relative humidity controlled at about 45% ± 5%, fed with standard solid composite feedstuff, and received tap water ad libitum as previously described.[8]

## Main apparatus and reagents

The main apparatus and reagents used in this experiment were an atomic absorption spectrophotometer (HG-9602A, Shenyang Huaguang Precise Instrument Co., Ltd), a transmission electron microscope (TEM; Sujing Group Antai Co., Ltd), and an iron normostock solution (500 mg/L, Institute for Reference Materials of SEPA).

## Preparation of $Fe_3O_4$ NMPs

As described previously,[9] we dissolved a quantity of ferric chloride hexahydrate (0.02 mol/L) and ferrous sulfate heptahydrate (0.012 mol/L) in 200 mL of deionized water under nitrogen protection. Ammonium hydroxide 25% was then added slowly with vigorous magnetic force stirring until pH was 9. The procedure took 30 minutes to generate a dark precipitate. Next, we separated the resultant with a permanent magnet and washed this repeatedly with deionized water 5–7 times until the pH of the supernatant was 7. Finally, the resultant was lyophilized and observed under TEM.

## Experimental group

Forty-two ICR mice were divided into two groups. Thirty-six mice were divided (n = 6) into A, B, C, D, E, and F experimental groups, given 600 mg/kg $Fe_3O_4$ MNPs by intragastric administration, and fed a normal diet. Another six control mice were given 0.5 mL of sterile physiologic saline by intragastric administration and also fed a normal diet.

## Preparation of sample

After intragastric administration, 0.2–0.5 mL of blood from one mouse in each group were collected into an ethylenediaminetetraacetic acid tube by enucleating eyeballs at the time points of zero minutes, hours 1, 3, 5, 6, and 7, and days 1, 3, 5, 7, and 10. The mice were then sacrificed by cervical dislocation, and samples of heart, liver, spleen, lungs, kidneys, bone marrow, brain, stomach, and small intestine were collected. After removing the fatty and connective tissue on the joint, the remaining tissues were washed with physiologic saline, dried with filter paper, and weighed to determine $Fe_3O_4$ MNP content.

## Distribution and concentration of $Fe_3O_4$ NMPs

Tissue samples of heart, liver, spleen, lungs, kidney, brain, stomach, and small intestine were freeze-dried and digested using microwave digestion with a $HNO_3$-$HClO_4$(V:V = 5:1) acid mixture. Each digested sample (0.2 g) was diluted to 50 mL with deionized water, while the heparinized blood was diluted in 0.02% Triton X-100 and 0.02% $HNO_3$. The iron elements of the spectrum were absorbed by iron atoms of the sample steam, and iron content in the sample was determined using atomic absorption spectrophotometry.

# Results

## Morphology and appearances

The size and appearance of the $Fe_3O_4$ MNPs were examined by TEM. Figure 1 shows representative images of the spinel ferrite compounds, which were spherical with a narrow diameter distribution, and the average particle size observed under TEM was 20 nm after being lyophilized (Figure 1).

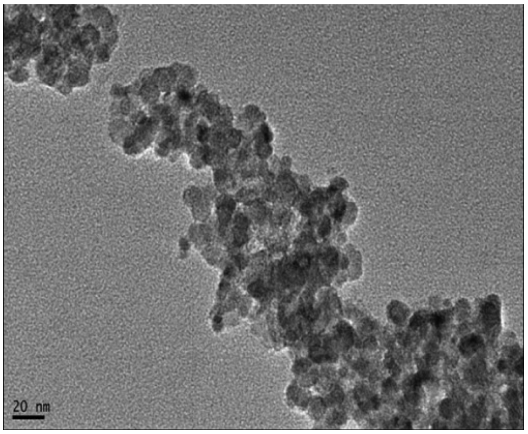


**Figure 1** Image of magnetic nanoparticles of $Fe_3O_4$ under transmission electron microscope. Bar = 20 nm (40,000×).

## General condition of mice

Mice in the control group were all in good condition and were agile, responsive, and covered with soft and glossy hair. Their consumption of water and food was normal, and their stool was formed and yellowish-brown. Those treated with $Fe_3O_4$ MNPs showed less activity and gathered together with enhanced resistance, and had slightly disordered hair. They ate and drank a little less, but all survived for the duration of monitoring.

## Blood concentration of $Fe_3O_4$ MNPs at different time points

The results of atomic absorption spectrophotometry showed that the highest concentration of $Fe_3O_4$ MNPs in the peripheral blood of mice was 439 ± 28 μg/mL at six hours in the experimental group after intragastric dosing, and decreased slowly but remained at a higher level until it reached another distribution peak of 436 ± 32 μg/mL on day 5 and then gradually declined again. During the entire observation period, the concentration of $Fe_3O_4$ MNPs in the experimental group at particular time points was higher than that of the control group, and there were significant differences between the groups ($P < 0.05$, Figure 2).

## Distribution of $Fe_3O_4$ MNPs in various organs and tissues

The distribution of $Fe_3O_4$ MNPs in the various organs and tissues is shown in Figures 3 and 4. By comparing the concentrations of $Fe_3O_4$ MNPs at all time points between the experimental and control groups, there were statistically significant differences in heart and bone marrow tissue distribution ($P < 0.05$) in the liver and small intestine on days 1, 3, and 7; in the spleen and brain on days 1 and 3; in the lungs at six hours; in the kidneys at six hours and on day 1; and in the stomach from six hours to day 7 after administration, suggesting that $Fe_3O_4$ MNPs are distributed widely in various organs in vivo, including the heart, liver, spleen, lungs, kidneys, bone marrow, brain, stomach, and small intestine. Furthermore, we also found that the peak distribution of $Fe_3O_4$ MNPs in various organs and tissues was different. There were two distribution peaks in the liver. The first distribution peak was on day 1 and then decreased gradually until it reached a second peak on day 7 after administration. The second peak concentration of $Fe_3O_4$ MNPs was 208 ± 16 μg/g and was slightly lower compared with day 1, but there was no significant difference between the two peak values ($P > 0.05$). While the concentration of $Fe_3O_4$ MNPs in the heart or spleen increased gradually with the passage of

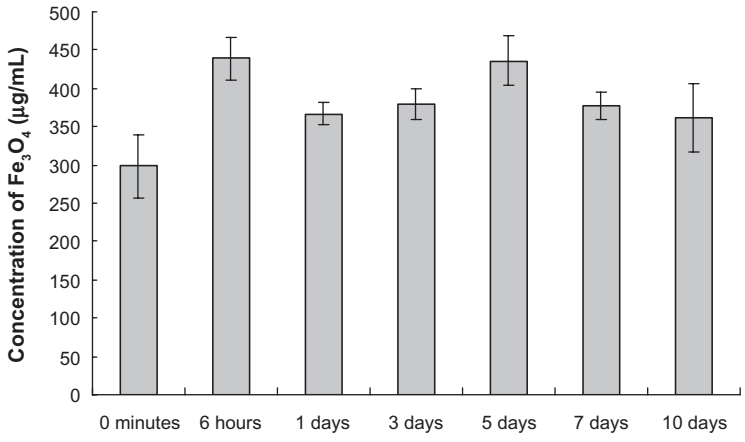


**Figure 2** Concentration of $Fe_3O_4$ MNPs in peripheral blood of mice (n = 6).

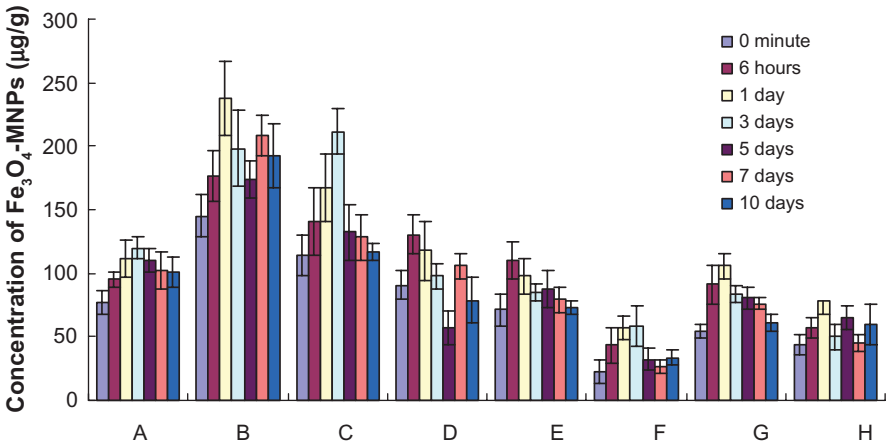


**Figure 3** The concentrations of $Fe_3O_4$ MNPs in tissues of mice (n = 6). **A** heart, **B** liver, **C** spleen, **D** lungs, **E** kidneys, **F** brain, **G** stomach, and **H** small intestine.

time, the peak values were 119 ± 9 μg/g and 211 ± 18 μg/g, respectively, on day 3 after dosing. The value in the lung was 131 ± 15 μg/g at six hours after dosing, and then decreased steadily. Levels in both kidneys also peaked six hours after dosing, and decreased gradually to a small degree. Brain levels rose rapidly after dosing, achieved a peak value of 58 ± 16 μg/g on day 3, and thereafter decreased gradually. Meanwhile, peak stomach, small intestine, and bone marrow levels were reached on day 1, with respective peak values of 106 ± 10 μg/g, 79 ± 11 μg/g, and 1.97 ± 0.12 μg/g. Interestingly, concentrations of $Fe_3O_4$ MNPs were higher in the liver and spleen than those in other organs. Maximum uptake in the liver was 237 ± 29 μg/g, reached on day 1, and that in the spleen was 211 ± 18 μg/g, reached on day 3 after dosing, indicating that the liver and spleen were the main distribution tissues and are the probable target organs for $Fe_3O_4$ MNPs.

## Discussion

Iron is an essential element, widely distributed in the body, and primarily involved in oxygen transport and utilization. Almost all organs contain iron in vivo, but the most highly ferruginous organs are the liver and spleen, and the lungs also contain considerable amounts of iron.[10] Iron metabolism in the body is a relatively closed system[11,12] and there is very little loss of body iron in normal circumstances compared with metabolism of other materials.[13] Human cells lack an excretion mechanism for iron under physiologic conditions and, therefore, iron balance in the body is regulated by absorption of dietary iron through the small intestine. $Fe_3O_4$ MNPs have a diameter of less than 100 nm. The physical and chemical properties of iron when being made into nanoparticles and the iron metabolism model in vivo would also be different from that of normal ferric iron.

From the results of our experiment, we can see that there is a close relationship between the blood concentration-time changes for $Fe_3O_4$ MNPs and changes in their tissue concentrations in the liver and spleen. A large number of $Fe_3O_4$ MNPs were ingested by mononuclear macrophages in the liver or spleen after being absorbed into the blood, with a distribution peak in blood of 439 ± 28 μg/mL at six hours. As a result, the concentration of $Fe_3O_4$ MNPs in blood declined rapidly, while that in the liver and spleen reached highest levels on days 1 and 3, respectively. Thereafter, the liver and spleen released ferric iron which participated in the cycle of iron metabolism in vivo, resulting in a decreased concentration of $Fe_3O_4$ MNPs in the liver and spleen (mainly spleen). An increased concentration of $Fe_3O_4$ MNPs in peripheral blood was observed up to the distribution peak at day 5 after administration. With the gradual senescence of red blood cells and impaired absorption in the liver and spleen (mainly the liver), the concentration of $Fe_3O_4$ MNPs in the liver increased again and reached a second distribution peak of 208 ± 16 μg/g on day 7, while

**Table 1** Concentration of magnetic $Fe_3O_4$ nanoparticles in bone marrow of mice (n = 6 ± standard deviation)

| Times concentration (μg/mL) | | |
|---|---|---|
| 0 minute | 0.49 ± 0.08 | |
| 6 hours | 1.03 ± 0.13 | |
| | 1 day | 1.97 ± 0.12 |
| | 3 days | 1.96 ± 0.10 |
| | 5 days | 1.40 ± 0.24 |
| | 7 days | 1.00 ± 0.14 |
| | 10 days | 0.81 ± 0.16 |

that in peripheral blood decreased gradually. Under normal circumstances, about 80% of iron is combined with plasma transferrin, and enters the bone marrow and participates in the synthesis of reticulocytes.[15] About four to six days later, this iron goes into the circulation again, leading to increased iron content in the blood.[11] In this experiment, the changes in concentration of $Fe_3O_4$ MNPs in the peripheral blood of mice were consistent with those reported by Moore et al.[15] The concentration of $Fe_3O_4$ MNPs in the kidney remained slightly above the background level during the entire observation period, indicating that renal excretion of iron is modest, which is consistent with a report by Pouliquen et al.[16]

In this study, there was a significant difference in brain tissue concentrations of $Fe_3O_4$ MNPs between the experimental and control groups, indicating that $Fe_3O_4$ MNPs can penetrate the blood–brain barrier. The blood–brain barrier is composed of a layer of endothelial capillary cells between the blood and the brain, where these cells connect tightly on the one hand to prevent invasion by exogenous pathogens and, on the other hand, form an obstacle which is hard to cross in terms of drug and gene delivery. It is likely that utilization of $Fe_3O_4$ MNPs as drug carriers may overcome the physiologic limitations of drug transport by capillary barriers.[17] Currently, the mechanism by which nanoparticles traverse the barrier is unclear.[18] Although iron oxide nanoparticles are known to be well tolerated by the body and degrade with time,[19] it is worthwhile verifying whether the structure of $Fe_3O_4$ MNPs changes after digestion and absorption through the intestine. Hence, we need to investigate further their potential to cause chronic long-term harm in the human body.

## Conclusions

This study of the pharmacokinetics and tissue distribution of magnetic $Fe_3O_4$ nanoparticles in ICR mice showed that these nanoparticles were mostly taken up in the liver and spleen, so the curative effect could be more pronounced for tumors in the liver. Furthermore, $Fe_3O_4$ MNPs can penetrate the blood–brain barrier, so they might be used as drug carriers to overcome the limitations of physiologic barriers.

## Acknowledgments

This work was supported by the 973 National Key Fundamental Research Project of China (Number 2006CB933205), 863 Project of the People's Republic of China (Number 2007AA022007), National Nature Science Foundation of the People's Republic of China (Numbers 30740062, 30872970), and the Special Purpose Science Research Foundation for High Schools (Number 20070286042).

## Disclosure

The authors report no conflicts of interest relevant to this study.

## References

1. Li ZQ, Chen ZM. Preparation characterization and application of nano magnetic polymer materials. *Chem Ind Times*. 2007;21(6):57–60.
2. Singh R, Lillard JW. Nanoparticle-based targeted drug delivery. *Exp Mol Pathol*. 2009;86(3):215–223.
3. Bourrinet P, Bengele HH, Bonnemain B, Dencausse A, Idec JM, Jacobs PM. Preclinical safety and pharmacokinetic profile of Ferumoxtran-10, an ultrasmall superparamagnetic iron oxide magnetic resonance contrast agent. *Invest Radiol*. 2006;41(3):313–324.
4. Neuberger T, Schöpf B, Hofmann H, Hofmann M, von Rechenberg B. Superparamagnetic nanoparticles for biomedical applications: Possibilities and limitations of a new drug delivery system. *J Magn Magn Mater*. 2005;293(1):483–496.
5. Chen BA, Cheng J, Wu YN, et al. Reversal of multidrug resistance by magnetic $Fe_3O_4$ nanoparticle copolymerizating daunorubicin and 5-bromotetrandrine in xenograft nude-mice. *Int J Nanomedicine*. 2009;4(1):73–78.
6. Chen BA, Cheng J, Shen MF, et al. Magnetic nanoparticle of $Fe_3O_4$ and 5-bromotetrandrin interact synergistically to induce apoptosis by daunorubicin in leukemia cells. *Int J Nanomedicine*. 2009;4(1):65–71.
7. Powers KW, Palazuelos M, Moudgil BM. Characterization of the size, shape, and state of dispersion of nanoparticles for toxicological studies. *Nanotoxicology*. 2007;1(1):142–151.
8. Chen BA, Lai BB, Cheng J, et al. Daunorubicin-loaded magnetic nanoparticles of $Fe_3O_4$ overcome multidrug resistance and induce apoptosis of K562-n/VCR cells *in vivo*. *Int J Nanomedicine*. 2009;4:201–208.
9. Jain PK, Morales MA, Sahoo SK, Leslie-Pelecky D, Labhasetwar V. Iron oxide nanoparticles for sustained delivery of anticancer agents. *Mol Pharm*. 2005;2(3):194–205.
10. Kaufman CL, Williams M, Ryle LM, Smith TL, Tanner M, Ho C. Superparamagnetic iron oxide particles transactivator protein-fluorescein isothiocyanate particle labeling for in vivo magnetic resonance imaging detection of cell migration: Uptake and durability. *Transplantation*. 2003;76(7):1043–1046.
11. Sun S, Zeng H, Robinson DB, Genove G, Morel PA. Monodisperse $MFe_2O_4$ (M = Fe, Co, Mn) nanoparticles. *J Am Chem Soc*. 2004;126(1):273–279.
12. Ahrens ET, Feili-Hariri M, Xu H, et al. Receptor-mediated endocytosis of iron-oxide particles provides efficient labeling of dendritic cells for in vivo MR imaging. *Magn Reson Med*. 2003;49(6): 1006–1013.
13. Jing M, Liu XQ, Liang P, et al. Labeling neural stem cells with superparamagnetic iron oxide in vitro and tracking after implantation with MRI *in vivo*. *Chin Med J*. 2004;84(16):1386–1389.
14. Dodd CH, Hsu HC, Chu WJ, et al. Normal T-cell response and in vivo magnetic resonance imaging of T cells loaded with HIV transactivator-peptide-derived superparamagnetic nanoparticles. *J Immunol Methods*. 2001;256(1–2):89–105.

15. Moore A, Grimm J, Han B, Santamaria P. Tracking the recruitment of diabetogenic CD8(+)T-cells to the pancreas in real time. *Diabetes*. 2004;53(6):1459–1466.
16. Pouliquen D, Gallois Y. Physicochemical properties of structured water in human album in and gammaglobulin solutions. *Biochimie*. 2001; 83(9):891–898.
17. Leonard F, Kulkarni RK, Brandes G, et al. Synthesis and degradation of poly(alkyl α-cyanoacrylate). *J Appl Polym Sci*. 1966;10(2):259–272.
18. Lockman PR, Koziara J, Roder KE, et al. *In vivo* and *in vitro* assessment of baseline blood-brain barrier parameters in the presence of novel nanoparticles. *Pharm Res*. 2003;20(5):705–713.
19. Okon E, Pouliquen D, Okon P, et al. Biodegradation of magnetite dextran nanoparticles in the rat. A histologic and biophysical study. *Lab Invest*. 1994;71:895–903.